IEEE Access
Multidisciplinary | Rapid Review | Open Access Journal

Received January 15, 2019, accepted February 6, 2019, date of publication February 18, 2019, date of current version March 18, 2019.

Digital Object Identifier 10.1109/ACCESS.2019.2899883

An Energy-Efficient Signal Detection Scheme for a Radar-Communication System Based on the Generalized Approximate Message-Passing Algorithm and Low-Precision Quantization

DE-PING XIA[1,2], YU ZHANG[3], (Senior Member, IEEE), PEIXIANG CAI[3], AND LING HUANG[4]

[1]National Laboratory of Radar Signal Processing, Xidian University, Xi'an 710071, China
[2]Nanjing Research Institute of Electronics Technology, Nanjing 210039, China
[3]Department of Electronic Engineering, Tsinghua University, Beijing 100084, China
[4]China Fortune Land Development Industrial Investment Co. Ltd., Beijing 100027, China

Corresponding author: Ling Huang (amyling99808@163.com)

This work was supported by the National Natural Science Foundation of China under Grant 91738202.

ABSTRACT Integrated radar-communication systems will play an important role in the future battlefield scenarios by decreasing the interference, volume, weight, and power consumption of equipment and promoting information fusion with an enhanced network. An active electronically scanned array radar system is ideal for such scenarios. However, a few studies have focused on the modeling and detection of communication signals for such integrated systems. In this paper, an array division strategy is developed, and a low-complexity signal detection scheme based on the generalized approximate message-passing (GAMP) algorithm is implemented. Furthermore, a quantization model is introduced into the output function of the GAMP algorithm. The method effectively provides communication signal detection with low-precision quantization and outperforms the linear minimum mean square error-based algorithm at the same precision levels. Overall, an energy-efficient radar-communication strategy is developed to promote the application of such systems in the future battlefield scenarios.

INDEX TERMS Integrated radar-communication system, GAMP algorithm, low-precision quantization algorithm, energy efficient.

I. INTRODUCTION

In the future integrated battlefield of sea, land, air and space, military platforms such as tanks, airplanes, and ships will be loaded with diverse electronic devices to enhance their interoperability and probability of survival [1], [2]. Various problems, such as interference, volume, weight, and power consumption issues, linked to these electronic devices will become increasingly serious [3], [4]. An integrated radar-communication system can largely alleviate or even solve the above problems by sharing hardware resources such as antennas and radio frequencies [5], [6]. Determining how to integrate radar and communication systems is crucial for improving the comprehensive performance of military platforms.

The associate editor coordinating the review of this manuscript and approving it for publication was Qinghua Guo.

Active electronically scanned array (AESA) radar has a flexible radio frequency (RF) beamforming capability and multifunction parallel execution capability [7]; therefore, it is suitable for the carrier platform in integrated radar-communication systems. AESA radar was used to conduct communication experiments in [8] and [9], but there is little research on system design and modeling for simultaneously employed radar and communication functions.

In fact, since the communication signal and the radar echo are received through the same antenna array, it is necessary to reasonably divide the array. On the one hand, the integrated radar-communication system must communicate with many objects in different directions to establish a complex communication network. On the other hand, the influence on radar detection performance due to the use of some antenna elements for communication should be minimized. Therefore, based on AESA radar, this paper designs a method

for dividing an array used by an integrated system, namely, the single antenna array elements that are not used by the radar system are selected for communication. The spacing of these antennas must be sufficiently large, typically more than a dozen wavelengths, to ensure that multiple independent signals can be received. Thus, the array elements used for communication signal receiving can reach tens or even thousands in communication systems for multiple antennas.

As the number of array elements increases, the communication performance improves; however, higher requirements are imposed on the signal detection scheme. Conventional detection schemes require pseudo-inverse operations involving the filter matrix, which is highly complex when the antenna array size is large [10], [11], resulting in a significant increase in the power consumption and the degradation of the overall performance of the integrated system. For the communication signal detection problem involving an integrated system, it is essential to develop a new signal detection scheme.

The generalized approximate message-passing (GAMP) algorithm replaces high-dimensional integrals with matrix-vector multiplication based on Gaussian approximation and the central limit theorem, thereby reducing the computational complexity [12]. Through a reasonable division and design of the integrated system based on AESA radar, this paper proposes a signal detection scheme based on the GAMP algorithm that uses the information from the prior probability distribution of the signal and the characteristics of the discrete distribution to effectively reduce the computational complexity of communication signal detection, power consumption, and overhead, improve the overall performance of the integrated system.

Furthermore, considering the structure of the AESA radar which has an RF link for each antenna, when the high-precision analog-to-digital converter is used in the RF chain, the power consumption of the circuit increases greatly [13]. Therefore, this paper adds a low-precision quantization operation to the system model. The improved GAMP algorithm is used for detection and updates the output function based on the comprehensive effect of Gaussian white noise superposition and quantization operations. This approach effectively restores data under low-precision quantization conditions and thus reduces the power consumption. The simulation results indicate that the detection scheme based on the GAMP algorithm can reduce the computational complexity and power consumption required for communication without sacrificing detection performance for both high-precision and low-precision quantization systems.

The remainder of this manuscript is organized as follows. Section II introduces the general problems in signal detection, including the system model and the traditional linear minimum mean square error (LMMSE) algorithm. Then, a signal detection scheme based on the GAMP algorithm is proposed, and an analysis of the corresponding complexity is presented. Section III describes the quantitative system model and gives the low-precision quantization model. Moreover, the specific improvement scheme is discussed in detail. The performance of the proposed scheme is verified by simulations in Section IV. Section V summarizes the main content of this article.

II. SIGNAL DETECTION BASED ON THE GENERALIZED APPROXIMATE MESSAGE-PASSING ALGORITHM

A. AN INTEGRATED COMMUNICATION AND DETECTION SYSTEM BASED ON AN AESA

Each front antenna channel unit of the AESA has a high-power amplifier or a low-noise amplifier and corresponding transmitter or receiver (T/R) components. The T/R components of each antenna channel can generate or receive wireless signals by themselves [14], with flexible beamforming and multifunction parallelism capability, therefore, simultaneous detection and communication functions can be performed through the division of the array [15].

The array division strategy is of great importance in a radar-communication system since the radar echo and the communication signal are transmitted and received through the same array. As a result, unsuitable divisional strategy can result in the degradation of the radar performance. There are quite a few studies which focus on the design of array division. For example, the division in subarrays is performed by the multi-objective genetic algorithm in [16] and [17] adopts the Pareto order genetic algorithm to implement the array division.

In the proposed multi-object transmission scenarios in this paper, we intend to use the GAMP algorithm to detect the communication signal with little influence on the radar detection performance. Therefore, there are two principles to select the single antenna array elements for communication: 1) The selected antenna array elements are not used by radar. 2) The spacing of these antennas is far enough to ensure that the data received by each antenna can be considered as independent.

The array division methods should be flexible with real-time application requirements. We adopt the signal detection scheme based on the GAMP algorithms because it is effective as long as the aforementioned two principles are satisfied, regardless of the detailed structure of array division methods.

A possible subarray partitioning diagram is shown in Fig. 1. Notably, the diagram depicts a special case in which the subarray has only one antenna and the single antenna transmits and receives in an omnidirectional manner.

The architecture of the integrated communication-detection system based on the AESA is shown in Fig. 2. The working modes of each module are as follows.

(1) In terms of signal generation and processing, the detection system and the communication system are two independent modules. When the corresponding task is generated, the task scheduler must allocate the corresponding resources.

(2) The task scheduler module is responsible for comprehensively sorting the requested tasks and allocating time, array and other resources for each task.

(3) After the task resources are reasonably allocated, the AESA RF front and antennas are connected so that the

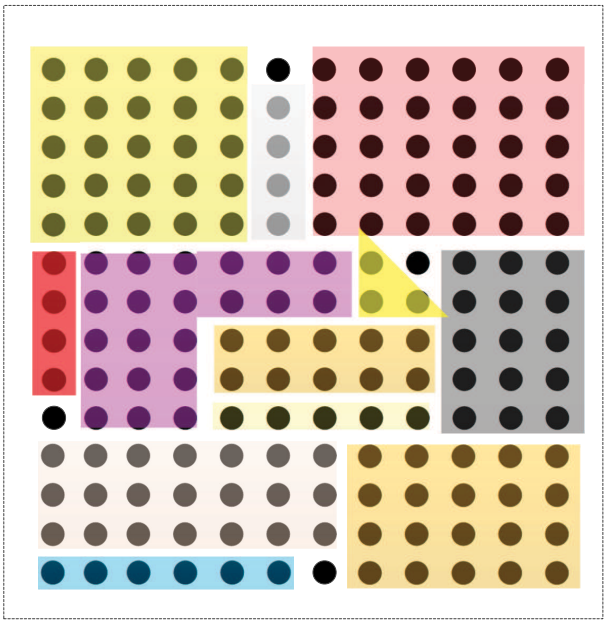

FIGURE 1. A schematic diagram of the subarray. The black dots indicate the antennas, and the antennas covered by the same color form a subarray. The single antennas are not covered by the color pattern.

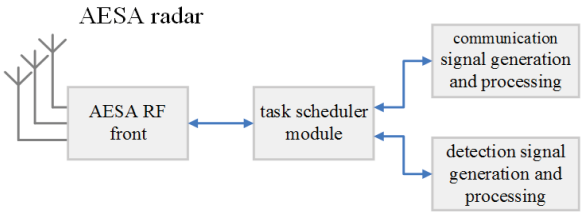

FIGURE 2. The architecture of the integrated detection and the communication system based on an AESA.

antenna array is assigned to each task to complete data transmission and reception.

In communication signal generation and processing, the modules for decoding, interleaving, synchronization, modulation, demodulation and equalization are loaded. In detection signal generation and processing, the modules for pulse compression, coherent processing, and miscellaneous wave suppression are loaded.

To transmit and receive communication signals with multiple objects in various direction, single antennas with sufficient spacing in the AESA radar are selected for receiving multiple communication data streams, as shown in Fig. 3. In practical application scenarios, the number of communication objects is quite large, and can reach dozens or even hundreds. Besides, the communication objects are widely distributed. This paper assumes that the signals transmitted by the communication objects are distributed in all directions with almost equal energy.

B. TRANSMISSION MODEL

Assuming that the receiver uses N_{R} antennas for receiving communication signals. Note that the receiving antennas may be unevenly distributed, but sufficiently spacing between the antennas must be ensured for independent signal receiving. There are K transmitting systems, the kth ($k = 1, \cdots, K$) transmitting system has n_{t}^k transmitting antennas that transmit independent data streams. For the receiver, the equivalent data streams N_{T} to be received is

$$N_{\mathrm{T}} = \sum_{k=1}^{K} n_{\mathrm{t}}^k. \tag{1}$$

Generally, $N_{\mathrm{T}} < N_{\mathrm{R}}$. Assuming that the received signals are evenly distributed in all spatial directions with approximately equal energy, and ensuring that the spacing of the receiving antennas is sufficiently large, then the data received through the antennas can be considered irrelevant. $\mathbf{H} \in \mathbf{C}^{N_{\mathrm{R}} \times N_{\mathrm{T}}}$ represents the fading channel between the transmitting and receiving antennas, and the element h_{ij} represents the channel condition between the jth transmitting antenna and the ith receiving antenna, which is based on a Gaussian distribution, i.e., $h_{ij} \sim N(0, 1/N_{\mathrm{R}})$. It is assumed that the channel state information $\mathbf{H}$ has been obtained. The channel is statically invariant during the coherence time, and L_{data} represents the length of the data transmitted during a coherence period, so the received signal of the ith receiving antenna can be expressed as follows.

$$\mathbf{r}_i = \sum_{j=1}^{N_{\mathrm{T}}} h_{ij}\mathbf{x}_j + \mathbf{w}, \tag{2}$$

where h_{ij} is the channel condition between the jth transmitting antenna and the ith receiving antenna, and $\mathbf{x}_j = [x_j^1\ x_j^2\ \cdots\ x_j^{L_{\mathrm{data}}}]$ represents the data transmitted by the jth transmitting antenna during a coherence period. Thus, transmitted data matrix $\mathbf{X}$ is

$$\mathbf{H} = \begin{bmatrix} \begin{pmatrix} x_1^1 & x_1^2 & \cdots & x_1^{L_{\mathrm{data}}} \\ \vdots & & & \\ x_{n_{\mathrm{t}}^1}^1 & x_{n_{\mathrm{t}}^1}^2 & \cdots & x_{n_{\mathrm{t}}^1}^{L_{\mathrm{data}}} \end{pmatrix}_{n_{\mathrm{t}}^1 \times L_{\mathrm{data}}} \\ \vdots \\ \begin{pmatrix} x_1^1 & x_1^2 & \cdots & x_1^{L_{\mathrm{data}}} \\ \vdots & & & \\ x_{n_{\mathrm{t}}^k}^1 & x_{n_{\mathrm{t}}^k}^2 & \cdots & x_{n_{\mathrm{t}}^k}^{L_{\mathrm{data}}} \end{pmatrix}_{n_{\mathrm{t}}^k \times L_{\mathrm{data}}} \\ \vdots \\ \begin{pmatrix} x_1^1 & x_1^2 & \cdots & x_1^{L_{\mathrm{data}}} \\ \vdots & & & \\ x_{n_{\mathrm{t}}^K}^1 & x_{n_{\mathrm{t}}^K}^2 & \cdots & x_{n_{\mathrm{t}}^K}^{L_{\mathrm{data}}} \end{pmatrix}_{n_{\mathrm{t}}^K \times L_{\mathrm{data}}} \end{bmatrix}_{N_{\mathrm{T}} \times L_{\mathrm{data}}}, \tag{3}$$

where the data transmitted by the antennas of all transmitting systems is represented by $x_{n_{\mathrm{t}}^k}^{L_{\mathrm{data}}}$. The M-order quadrature amplitude modulation (M-QAM) symbols are independently and identically distributed. The constellation of the M-QAM is ruled by,

$$\mathbf{A} = \mathrm{X_m} \times \{\pm(2k_{\mathrm{R}} + 1) \pm i(2k_{\mathrm{R}} + 1)\},$$
$$k_{\mathrm{I}}, k_{\mathrm{R}} \in [0, 2, \cdots, \sqrt{M}/2], \tag{4}$$

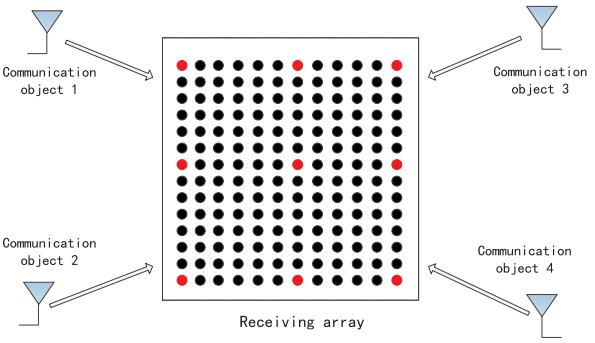

FIGURE 3. A schematic diagram of a multi-object transmission scenario based on an integrated detection and communication system. The black dots in the figure represent the antennas used by radar, and the red dots represent the single antennas for receiving the multiple data streams.

where M is the modulation order and X_m is the power normalization factor; for instance, for 64-QAM, $X_m = \sqrt{42}$.

We assume that the power of all transmitted signals is 1. $\mathbf{W} \in \mathbf{C}^{N_R \times L_{data}}$ is the additive complex White Gaussian noise with a variance of σ^2. The complex signal obtained at the receiver is,

$$\mathbf{R} = \mathbf{HX} + \mathbf{W}, \tag{5}$$

where $\mathbf{R} \in \mathbf{C}^{N_R \times L_{data}}$.

Next, considering the practice system, the signal is separately received by I and Q, implementing the GAMP algorithm in the real number field is more in line with the actual situation. Hence, formulas (4)-(5) are converted to the real number field:

$$\mathbf{R}_r = \mathbf{H}_r\mathbf{X}_r + \mathbf{W}_r, \tag{6}$$

where $\Re(\cdot)$ and $\Im(\cdot)$ represent that the real and imaginary parts of the quantity in parentheses, respectively, so $\mathbf{H}_r = \begin{pmatrix} \Re(\mathbf{H}) & -\Im(\mathbf{H}) \\ \Im(\mathbf{H}) & \Re(\mathbf{H}) \end{pmatrix}$, $\mathbf{R}_r = \begin{pmatrix} \Re(\mathbf{R}) \\ \Im(\mathbf{R}) \end{pmatrix}$, $\mathbf{X}_r = \begin{pmatrix} \Re(\mathbf{X}) \\ \Im(\mathbf{X}) \end{pmatrix}$, and $\mathbf{W}_r = \begin{pmatrix} \Re(\mathbf{W}) \\ \Im(\mathbf{W}) \end{pmatrix}$.

Then, we can re-express formulas (4)-(6) as follows:

$$\mathbf{Y} = \mathbf{AS} + \mathbf{N}, \tag{7}$$

where $\mathbf{Y} = \frac{1}{\sqrt{N_T}}\mathbf{R}_r$, $\mathbf{A} = \frac{1}{\sqrt{N_T}}\mathbf{H}_r$, $\mathbf{S} = \mathbf{X}_r$, $\mathbf{N} = \frac{1}{\sqrt{N_T}}\mathbf{W}_r$, and the variance is $\tilde{\sigma}^2 = \frac{\sigma^2}{2N_T}$.

Next, we estimate $\mathbf{S}$ using the receiver data $\mathbf{Y}$. In the M-QAM constellation, the prior probability distribution is given as follows:

$$p_s(\mathrm{s}) = \frac{1}{M}\delta(\mathrm{s} - \mathbf{A}_k), \tag{8}$$

where $\delta(\cdot)$ is the Dirac function, s is an element of $\mathbf{S}$, and $\mathbf{A}_k$ is the kth element of the M-QAM symbol set $\mathbf{A}$. Equations (4)-(8) indicate that the prior probability of corresponding symbols is based on a uniform discrete distribution.

C. SIGNAL DETECTION BASED ON THE LMMSE ALGORITHM

In a traditional multi-input and multi-output communication system, the LMMSE algorithm is typically used for signal detection. The calculation process is as follows.

$$\hat{\mathbf{S}}_{\mathrm{LMMSE}} = (\mathbf{A}^H\mathbf{A} + \sigma^2\mathbf{I}_{N_R})^{-1}\mathbf{A}^H \cdot \mathbf{Y}, \tag{9}$$

where $\mathbf{A}^H$ is obtained from the conjugate transpose operation involving $\mathbf{A}$, $\mathbf{I}_{N_R}$ represents a unit matrix with N_R dimensions, and $(\cdot)^{-1}$ denotes that the variable in the parentheses is inverted. When K and N_T increases, which is common when communicating with multiple objects, the LMMSE algorithm results in extensive computations due to the matrix inversion operation, which may affect the performance of the radar. Therefore, a novel detection scheme is required to reduce the computational complexity.

D. SIGNAL DETECTION BASED ON THE GENERALIZED APPROXIMATE MESSAGE-PASSING ALGORITHM

GAMP is a factor graph inference algorithm for dense connections that was proposed by Sundeep Rangan et al. in 2012. It uses Gaussian approximation and the central limit theorem for large-scale systems to replace high-dimensional integrals with matrix-vector multiplication operations, so that the complexity of computations is reduced [12]. The GAMP algorithm is proposed to solve the signal recovery problem shown in Fig. 4. The input variable is $\mathbf{q} \in \mathrm{Q}^n$, and $\mathbf{x} \in \mathbf{R}^n$ is obtained by the input function, with conditional probability distribution $p_{X|Q}(x_j|q_j)$. $\mathbf{x}$ is transformed by the transformation matrix $\mathbf{A}$ to obtain $\mathbf{z} = \mathbf{Ax}$, and $\mathbf{z}$ is passed through the output function with conditional probability distribution $p_{Y|Z}(y_i|z_i)$ to sequentially obtain the system output vector $y \in \mathbf{Y}^m$. For the system, $\mathbf{q}$, $\mathbf{y}$, $\mathbf{A}$ and the two conditional probability distributions are known, whereas $\mathbf{x}$ and $\mathbf{z}$ must be estimated. Through the analyses of practical problems and an in-depth understanding of the GAMP algorithm, this paper uses the GAMP algorithm to solve the signal detection problem. There are two reasons why this algorithm is suitable. First, as theoretically derived in [12], the algorithm is applicable to estimation problems in which $\mathbf{x}$ obeys a discrete distribution, no matter $\mathbf{x}$ is a sparse vector or not. In fact, the discrete distribution is also essentially a sparse distribution. The communication symbols to be detected in this section are the discrete QAM symbols of the constellation, so the problem can be solved using the GAMP algorithm. Second, [12] showed that when the elements of linear transformation matrix $\mathbf{A}$ follow an

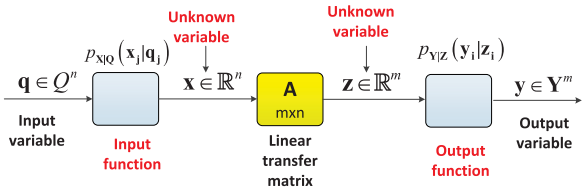

FIGURE 4. A schematic diagram of GAMP algorithm signal recovery model.

independent Gaussian distribution, the algorithm can guarantee convergence. The channel impulse response between each transceiver antenna in the system model follows this type of distribution, so the GAMP algorithm can be used to solve the corresponding signal detection problem. The above reasons ensure that GAMP algorithm can be adopted to solve the signal detection problem in this paper.

For the specific signal detection problem studied in this paper, the mathematical forms of the input and output functions based on the GAMP algorithm framework is presented as follows. According to the system model in (5), the input function is set as a deterministic function.

$$p_{X|Q}(x_j|q_j) = 1. \tag{10}$$

Moreover, the output function is set to a zero-mean additive white Gaussian noise function:

$$p_{Y|Z}(y_i|z_i) = \frac{1}{\sqrt{2\pi\sigma_w^2}}\exp(-\frac{(y-z)^2}{2\sigma_w^2}), \tag{11}$$

where σ_w is the variance of the Gaussian white noise in the output function. Then, a low-complexity signal detection scheme for multiple transmission objects is proposed based on GAMP algorithm.

The specific implementation process and the message-passing process is briefly discussed as follows. Based on the system model in Section II-A, $\mathbf{S}$ should be recovered from the received signal $\mathbf{Y}$. The row labels of the variables $\mathbf{Y}$ and $\mathbf{S}$ are $i \in [0, 2N_{\mathrm{R}}]$ and $j \in [0, 2N_{\mathrm{T}}]$,respectively, because both the real and imaginary parts should be calculated. In this case, the column labels are ignored for simplicity. Let the superscript t indicates the number of iterations, and the message, namely, the probability of passing between $\mathbf{S}$ and $\mathbf{Y}$, is shown in (12) and (13).

$$m^t_{y_i\leftarrow s_j}(s_j) \propto p_s \prod_{l\neq j} m^t_{y_l\rightarrow s_j}(s_j), \tag{12}$$

$$m^t_{y_i\rightarrow s_j}(s_j) \propto \int p_{y|as} \prod_{k\neq j} m^{t-1}_{y_i\leftarrow s_k}(s_j)ds_j. \tag{13}$$

In this paper, the result of $m^t_{y_i\leftarrow s_j}(s_j)$ is called the variable node update, and the result of $m^t_{y_i\rightarrow s_j}(s_j)$ is called the observation node update. The approximate edge distribution of the variable node is as follows.

$$\hat{p}^t_{s_j|Y}(s_j|Y) \propto p_s(s_j) \prod_{i=1}^{2N_{\mathrm{R}}} m^t_{y_i\rightarrow s_j}(s_j). \tag{14}$$

Therefore, the estimated value of s_j can be expressed as follows.

$$\hat{s}^t_j = \int s\hat{p}^t_{s_j|Y}(s_j|Y)ds. \tag{15}$$

The calculation process of equations (12) and (13) involves high-dimensional integrals that are very complicated. According to [12], when N_{T} and N_{R} are large, $m^t_{y_i\rightarrow s_j}(s_j)$ is an approximate Gaussian probability density distribution, and $m^t_{y_i\leftarrow s_j}(s_j)$ is the sum of the approximate Gaussian variables and the corresponding second-order perturbations. The associated mean and variance have simple forms for calculations. As a result, we can calculate the first-order and second-order statistical properties of $\mathbf{S}$ and $\mathbf{Y}$ to obtain the estimated values of $m^t_{y_i\rightarrow s_j}(s_j)$ and $m^t_{y_i\leftarrow s_j}(s_j)$.

Given the prior probability distribution p_s, the received observation matrix $\mathbf{Y}$, the channel state information $\mathbf{A}$, and the noise variance $\tilde{\sigma}^2$, the implementation of signal detection based on GAMP algorithm is as follows.

1. Initialization. Let the iteration number $t = 0$, and let $s = 0$. Set the iteration *threshold* to a sufficiently small value, and let

$$\hat{s}^0_j = EXP(s), \tag{16}$$

$$vs^0_j = VAR(s), \tag{17}$$

$$\hat{z}^0_i = \frac{1}{N_{\mathrm{T}}}. \tag{18}$$

Here, $EXP(\cdot)$ and $VAR(\cdot)$ are the expectation and the variance of the variable in parentheses, which are calculated according to the prior probability in (8).

2. Linear updating of observation nodes.

$$\hat{p}^t_i = \sum\nolimits_j a_{ij}\hat{x}^t_i - vp^t_i\hat{z}^{t-1}_i, \tag{19}$$

$$vp^t_i = \sum\nolimits_j a^2_{ij}vx^{t-1}_i. \tag{20}$$

3. Nonlinear updating of observation nodes.

$$\hat{z}^t_i = (y_i - p^t_i)/(vp^t_i + \tilde{\sigma}^2), \tag{21}$$

$$vz^t_i = 1/(vp^t_i + \tilde{\sigma}^2). \tag{22}$$

4. Linear updating of variable nodes.

$$\hat{r}^t_j = \hat{s}^{t-1}_j + vr^t_j \sum\nolimits_i a_{ij}\hat{z}^t_i, \tag{23}$$

$$vr^t_j = [\sum\nolimits_i a^2_{ij}vz^t_i]^{-1}. \tag{24}$$

5. Nonlinear updating of variable nodes.

$$\hat{s}^t_j = EXP[s|\hat{r}^t_j, vr^t_j], \tag{25}$$

$$vs^t_j = VAR[s|\hat{r}^t_j, vr^t_j]. \tag{26}$$

The mean and variance are calculated based on the probability distribution $p(s|\hat{r}^t_j, vr^t_j) \propto N(s; \hat{r}^t_j, vr^t_j)p_s(\cdot)$.

6. Termination condition. For each iteration result $t = 1, 2, 3, \cdots$, the estimation result $\hat{\mathbf{S}}^t$ of the real result $\mathbf{S}$ is the output. If the following condition is met

$$\frac{\|\hat{\mathbf{S}}^{t+1} - \hat{\mathbf{S}}^t\|_2}{\|\hat{\mathbf{S}}^t\|_2} \leq threshold, \tag{27}$$

where $\|\cdot\|_2$ represents the l_2 norm of the vector, then $\hat{\mathbf{S}}^{t+1}$ will be output as the final estimation result, and the iteration process stops. Otherwise, $t = t + 1$, and the algorithm returns to step 2 to continue the process until the termination condition is met.

E. COMPLEXITY ANALYSIS

The complexity of the signal detection scheme based on the GAMP algorithm is low because the operational process only adopts multistep iterations and matrix-vector multiplication rather than involving matrix inversion. For a detection process that transmits L_{data} data symbols in a given coherence time, the matrix multiplication mainly involves (19), (20), (23), and (24) in the proposed scheme, and the complexity of one iteration is $O(N_{\text{T}}N_{\text{R}}L_{\text{data}})$. The integral operation of the mean and variance in (25) and (26) seems complicated but is actually simple because the integral term includes the probability distribution $p(x|\hat{r}_j^t, vr_j^t) \propto N(x; \hat{r}_j^t, vr_j^t)p_x(\cdot)$, where p_s is a discrete distribution that can be determined from (8). Hence, the main computation complexity comes from multiplication operations, and other complexity such as the add operation can be ignored. $\bar{N}$ represents the total number of iterations when the termination condition is met; therefore, the computational complexity of the proposed scheme is $O(\bar{N}N_{\text{T}}N_{\text{R}}L_{\text{data}})$. When the number of transmitting and receiving antennas is large, the computational complexity of the detection scheme based on the GAMP algorithm can be reduced by an order of magnitude compared to the traditional LMMSE detection algorithm, which has a computational complexity of $O(N_{\text{T}}^3L_{\text{data}})$.

III. LOW-PRECISION QUANTIZATION SIGNAL DETECTION BASED ON THE GAMP ALGORITHM

A. SYSTEM MODEL

Since each antenna channel of the AESA radar corresponds to one RF link, and the signals received by each antenna are converted to discrete signals by an analog-to-digital converter (ADC) in the RF link. Then, signals are sent to the digital signal processor for analysis and calculations, as shown in Fig. 5. However, in the case of a large number of RF chains, the use of high-precision ADCs in the RF link results in high circuit power consumption [13]. Thus, this section considers the low-precision quantization problem of detection processing at the receiving end.

In this section, the GAMP algorithm is introduced into the receiver detection system for quantization operations.

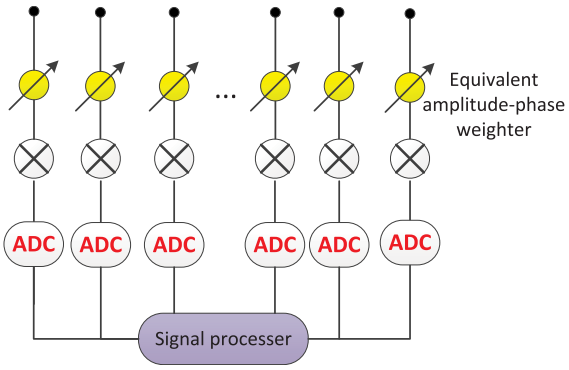

FIGURE 5. Receiver RF structure diagram.

In the case of low-precision quantization, the influence of the quantization operation is added to the output function, and the probability distribution of the output function is updated to recover the signal by probability estimation. The proposed scheme is compared with the LMMSE algorithm, which directly detects the quantized signal.

After quantization, the system model can be expressed as follows:

$$\mathbf{R}^{Q} = Q(\mathbf{HX} + \mathbf{W}), \tag{28}$$

where $\mathbf{R}^{Q}$ is the quantized data output at the receiving end and $Q(\cdot)$ is the quantization operation. The specific form of the quantizer will be introduced in the next section.

According to Section II-B, if the LMMSE algorithm is used to detect the quantized data $\mathbf{R}^{Q}$, the result is

$$\begin{aligned}\hat{\mathbf{S}}_{\text{LMMSE-Q}} &= (\mathbf{A}^H\mathbf{A} + \sigma^2\mathbf{I}_{N_{\text{R}}})^{-1}\mathbf{A}^H \cdot \mathbf{R}^{Q} \\ &= (\mathbf{A}^H\mathbf{A} + \sigma^2\mathbf{I}_{N_{\text{R}}})^{-1}\mathbf{A}^H \cdot Q(\mathbf{HX} + \mathbf{W}).\end{aligned} \tag{29}$$

This process was renamed the LMMSE-Q-based detection scheme.

B. LOW-PRECISION QUANTIZATION

For any element $c = c_r + i \times c_i$ in matrix $\mathbf{C}$, both the real c_r and imaginary parts c_i can be quantized by the quantizer. The b-bit uniform complex quantizer $Q(\cdot)$ used in this paper is constructed as follows:

$$r = Q(c) = \begin{cases} sign(c) \times (\left[\frac{c}{\Delta}\right]\Delta + \frac{\Delta}{2}), & |c| < G + \frac{\Delta}{2} \\ sign(c) \times G, & |c| \geq G + \frac{\Delta}{2} \\ \frac{\Delta}{2}, & c = 0 \end{cases} \tag{30}$$

where r is the quantized result of element c in matrix $\mathbf{C}$, $sign(\cdot)$is the sign function, $\Delta = \max(\mathbf{C})/2^{b-1}$ is the quantization step size, and $G = ([|\max(\mathbf{C})|/\Delta]) \cdot \Delta$ is the saturation level.

Since the power consumption of the ADC exponentially increases with the number of quantization bits, low-precision quantization in this paper mainly refers to reducing the number of quantized bits of the quantizer, i.e., the value of b. In the subsequent signal detection, it is necessary to obtain the upper bound B_{up} and lower bound B_{low} of the quantization interval for the quantization result r in (30).

$$B_{\text{up}}(r) = \begin{cases} +\infty, & r = G \\ r + \frac{\Delta}{2}, & else \end{cases} \tag{31}$$

$$B_{\text{low}}(r) = \begin{cases} -\infty, & r = -G \\ r - \frac{\Delta}{2}, & else \end{cases} \tag{32}$$

In addition, for the quantized data r, the function $q^{-1}(\cdot)$ required to obtain the upper and lower bounds of the

quantization interval is as follows.

$$q^{-1}(r) = \left[B_{\text{low}}(r), B_{\text{up}}(r)\right]. \tag{33}$$

C. LOW-PRECISION QUANTIZATION SIGNAL DETECTION BASED ON THE GAMP ALGORITHM

This section extends the signal detection scheme based on the GAMP algorithm to the detection of communication symbols of the integrated system with quantization. The output function, with a conditional probability density of $p_{Y|Z}(y_i|z_i)$, is updated to consider the comprehensive effect of the Gaussian white noise superimposed uniform quantizer, as denoted by the red box in Fig. 6.

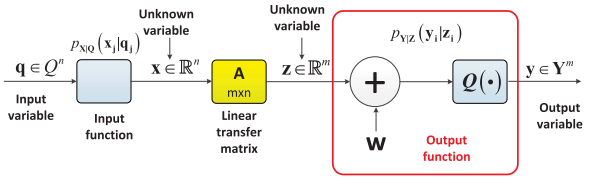

FIGURE 6. Schematic diagram of the output function added to the quantization operation in the GAMP algorithm framework.

The input function is the same as (10), and the output function is updated as follows.

$$p_{Y|Z}(y_i|z_i) = \int_{B_{\text{low}}(y)}^{B_{\text{up}}(y)} \frac{1}{\sqrt{2\pi\sigma_w^2}} \exp\left(-\frac{(t-z)^2}{2\sigma_w^2}\right) dt. \tag{34}$$

The GAMP algorithm extended to the integrated system with quantization is referred to as GAMP-quantization (GAMP-Q) algorithm. The implementation process of the GAMP-Q algorithm is the same as the GAMP-based algorithm in Section II-C, except that, in step 3, the nonlinear updating formulas of the observation nodes change to

$$\hat{z}_i^t = \frac{1}{vp_i^t + \tilde{\sigma}^2}\left(EXP[\zeta_i|\zeta_i \in q^{-1}(z_i)] - \hat{p}_i^t\right), \tag{35}$$

$$vz_i^t = \frac{1}{vp_i^t + \tilde{\sigma}^2}\left(1 - \frac{VAR[\zeta_i|\zeta_i \in q^{-1}(z_i)]}{vp_i^t + \tilde{\sigma}^2}\right). \tag{36}$$

In the formulas, the mean and variance are calculated according to the probability $\zeta_i \sim N(\hat{p}_i^t, vp_i^t + \tilde{\sigma}^2)$.

According to the above analysis, the increase in the computation complexity of GAMP-Q compared with GAMP is mainly reflected in (35) and (36). Although directly calculating the integral operations in (35) and (36) leads to high complexity, the integral content can be converted to a Gaussian error function $erf(\cdot)$, such as

$$erf(x) = \frac{2}{\pi}\int_0^x e^{-t^2} dt, \tag{37}$$

and the corresponding first, second and third derivatives, which can be quickly obtained using a look-up table. Therefore, this added complexity can be ignored, and the complexity of the GAMP-Q algorithm is the same as that of the GAMP algorithm, namely, $O(\bar{N}N_{\text{T}}N_{\text{R}}L_{\text{data}})$.

TABLE 1. Comparison Of The Complexity Of Different Schemes Based On The Gamp Algorithm And The LMMSE Algorithm.

N_{R}	N_{T}	16	64	128
128	$\bar{N}$	5.61	7.63	-
128	GAMP-based	3.45	18.75	-
128	LMMSE-based	1.23	78.64	-
256	$\bar{N}$	4.97	6.52	7.79
256	GAMP-based	6.11	32.05	76.58
256	LMMSE-based	1.23	78.64	629.15

The numbers in the table are $\times 10^6$.

IV. SIMULATION

A. SIGNAL DETECTION SCHEME BASED ON THE GAMP ALGORITHM

This section verifies the effectiveness of the proposed GAMP-based detection scheme through simulation results. Assuming that the channel remains unchanged during the coherence period, and the channel impulse response is known. For comparison, the modulation constellations are set to QPSK, 16QAM, and 64QAM. The simulation settings are as follows. The number of symbols transmitted in one coherence period L_{data} is set to 300. The signal-to-noise ratio (SNR) at the receiver is defined as $SNR = 10\log_{10}(N_{\text{R}}/\sigma^2)$. The numbers of transmitting and receiving antennas are set to N_{T} and N_{R}, respectively. The iteration termination condition is set to $threshold = 10^{-3}$. Each experiment involved 1000 independent runs, and the experimental data were averaged for comparison.

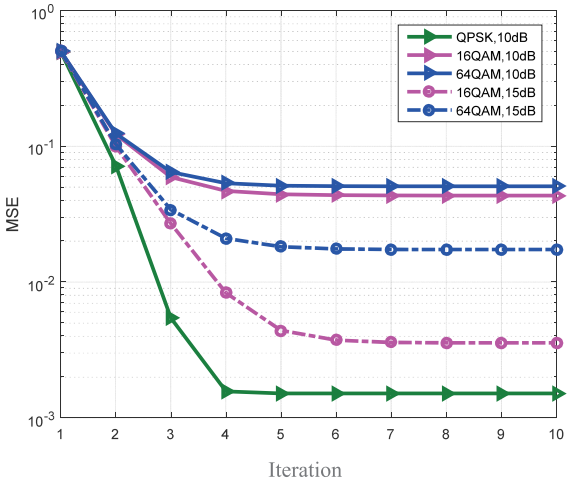

FIGURE 7. Simulation results of MSE with different iteration times in signal detection scheme based on GAMP algorithm.

Fig. 7 compares the mean square error (MSE) values, calculated by $\text{MSE}^t = \|\mathbf{S}^t - \mathbf{S}\|_2/2N_{\text{T}}L_{\text{data}}$, for different numbers of iterations, different modulation modes and different SNRs in the proposed GAMP-based signal detection scheme. The SNR is set to 10 dB and 15 dB, and the modulation methods are QPSK, 16QAM and 64QAM. The number of transmitting antennas is 32, and the number of receiving antennas is 128. The simulation compares the absolute error of the iteration results and the true value between each iteration.

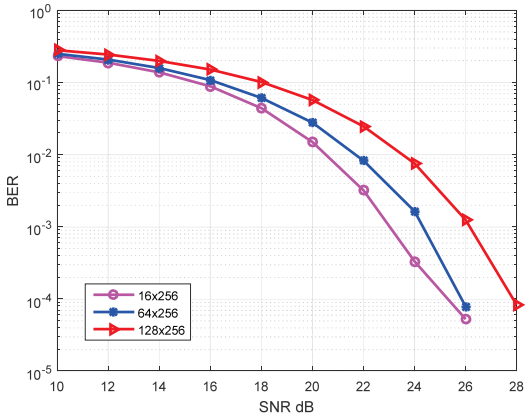

FIGURE 8. BER simulation results based on the GAMP Algorithm with different signal-to-noise ratios.

The GAMP algorithm can be stabilized by implementing only 8 to 10 iterations. When the numbers of transmitting and receiving antennas are large, the number of iterations is sufficiently small compared to the number of transmitting and receiving antennas; hence, the associated effect on complexity can be neglected. Therefore, the complexity of the signal detection scheme based on the GAMP algorithm can be considered as $O(N_{\mathrm{T}}N_{\mathrm{R}}L_{\mathrm{data}})$.

Table 1 shows a comparison of the complexities of the GAMP-based algorithm and the LMMSE-based algorithm when $L_{\mathrm{data}} = 300$. The table lists the average number of iterations $\bar{N}$ for the GAMP-based algorithm and the complexity of the two algorithms when N_{T} is 16, 64, and 128 and N_{R} is 128 and 256.

As shown in the table, when the number of transmitting and receiving antennas is large, the complexity of the GAMP-based scheme is significantly lower than that of the LMMSE-based algorithm. When $N_{\mathrm{T}} = 128$ and $N_{\mathrm{R}} = 256$, the complexity of the GAMP-based algorithm is 76.58×10^6, and the complexity of the LMMSE-based algorithm is 629.15×10^6. Additionally, when the number of transmitting antennas is not large, for instance, when $N_{\mathrm{T}} = 16$, the complexity of the GAMP-based algorithm is slightly higher than that of the LMMSE-based algorithm because the magnitudes of $\bar{N}$ and N_{T} are similar and N_{R} is much larger than N_{T}. Therefore, the GAMP-based algorithm is advantageous in the case in which the communication data stream is large. Combined with the results of the complexity analysis in the previous section, when the number of transmitting and receiving antennas is large, the GAMP-based scheme can significantly reduce the complexity by approximately an order of magnitude compared with the traditional LMMSE-based scheme.

The simulation results in Fig. 8 compare the bit error rate (BER) of the GAMP-based signal detection scheme with different SNRs for different numbers of transmitting and receiving antennas. The modulation mode is 64QAM; the number of transmitting antennas is 16, 64, and 128; and the number of receiving antennas is fixed at 256. If the number of receiving antennas is constant, the smaller the number of transmitting antennas is, the better the performance of the GAMP-based scheme. For example, if the BER is 10^{-3}, the performance of $N_{\mathrm{T}} = 16$ is improved by approximately 5% compared with $N_{\mathrm{T}} = 64$ and improved by approximately 13.2% compared with $N_{\mathrm{T}} = 128$. Notably, an increase in the number of transmitting antennas results in an increase in the system size.

In these cases, the difficulty and complexity of signal detection increases, resulting in a deterioration in performance. However, as the number of transmitting antennas increases, the detection results of the GAMP-based scheme remain superior.

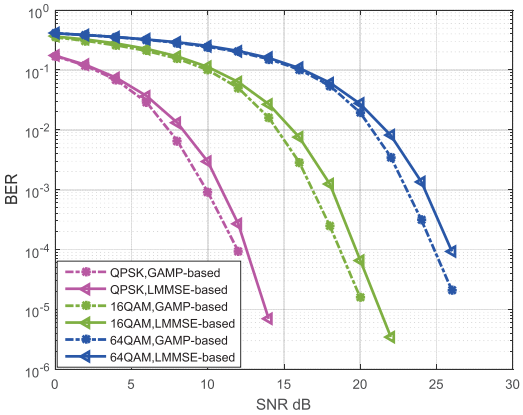

FIGURE 9. BER performance with different modulation order based on the GAMP and LMMSE algorithm.

The simulation results in Fig. 9 compare the BERs of the GAMP-based signal detection scheme and the LMMSE-based detection scheme for different SNRs and different modulation modes, including QPSK, 16QAM and 64QAM. The number of transmitting antennas is fixed at 32, and the number of receiving antennas is fixed at 128. Fig. 9 shows an increase in the modulation order leads to a decrease in the overall performance of both algorithms. For example, in the GAMP-based detection scheme, when the BER is 10^{-3}, the performance improvement of QPSK is approximately 41.4% compared with 16QAM and approximately 56.7% compared with 64QAM because the increase in the data detection rate results in a deterioration in communication quality. When the GAMP-based detection scheme is compared with the LMMSE-based detection scheme, we can conclude that when the SNR is low, the difference between the performance of the two schemes is small, whereas in the high-SNR scenarios, the GAMP-based detection scheme performs approximately 1 dB better than the LMMSE-based detection scheme. This performance difference occurs because the LMMSE algorithm treats the discrete signal probability distribution as a Gaussian distribution, and the GAMP algorithm accurately uses the prior probability distribution and the characteristics of the discrete distribution of the data. Therefore, using the GAMP-based scheme instead of the LMMSE-based scheme can improve the system detection performance.

B. LOW-PRECISION QUANTIZED SIGNAL DETECTION

This section illustrates the effectiveness of the GAMP-Q-based detection scheme in solving low-precision quantification problems through presenting simulation results.

We assume that the channel remains unchanged during the coherence period and that the channel impulse response has been obtained. To fully reflect the influence of quantization, a high-order modulation, namely, 256QAM, is adopted for data transmission. The number of symbols transmitted in the coherence period L_{data} is set to 300. The SNR at the receiving end is defined as $SNR = 10\log_{10}(N_{\text{R}}/\sigma^2)$, and the number of transmitting and receiving antennas are represented by N_{T} and N_{R}, respectively, which have different values. The iteration termination condition is set to $threshold = 10^{-3}$. The GAMP-Q-based detection scheme is compared with the LMMSE-Q-based detection scheme. Each simulation was performed with 1000 independent experiments, and the experimental data were averaged for comparison.

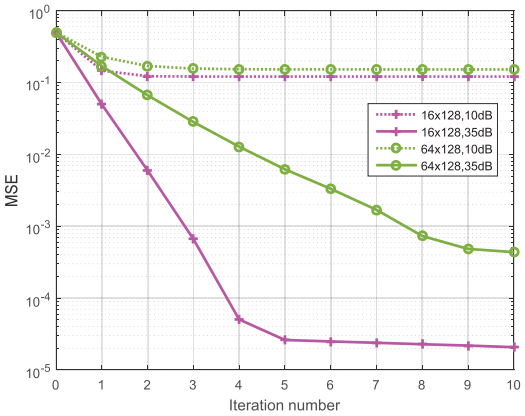

FIGURE 10. Simulation results of the mean square error of detection based on the GAMP-Q algorithm for different numbers of iterations.

The simulation results in Fig. 10 show the MSE of the low-precision GAMP-Q-based detection scheme for different numbers of iterations, different numbers of transmitting and receiving antennas and different SNRs. The calculation formula for the MSE is $\text{MSE}^t = \|\mathbf{S}^t - \mathbf{S}\|_2/2N_{\text{T}}L_{\text{data}}$. The SNR is given as 10 dB and 35 dB, and the quantization accuracy is 7 bits. The number of transmitting antennas is 16 and 64, and the number of receiving antennas is fixed at 128. As shown in Fig. 10, the convergence speed of the GAMP-Q-based scheme is very fast, and the algorithm converges in approximately 10 iterations. Additionally, the higher the SNR is, the smaller the MSE when the algorithm converges. For example, the MSE when the SNR is 35 dB is less than 10^{-3}, and when the SNR is 10 dB, the MSE is larger than 10^{-1}. Moreover, when the SNR is constant, the larger the difference between the number of transmitting and receiving antennas is, the faster the algorithm converges. When the SNR is 35 dB, the curve when $N_{\text{T}} = 16$ converges after 5 iterations, and the curve when $N_{\text{T}} = 64$ stabilizes after 10 iterations. However, ignoring the difference between the SNR and the numbers of transmitting and receiving antennas, the GAMP-Q-based scheme displays a fast convergence speed. When the total number of transmitting and receiving antennas is large, the number of iterations in the GAMP-Q-based scheme is small enough to be considered negligible when compared to the total number of antennas, and the computational complexity does not significantly increase compared to that of the GAMP-based algorithm. Notably, the complexity is reduced by an order of magnitude compared to that of the LMMSE-based algorithm.

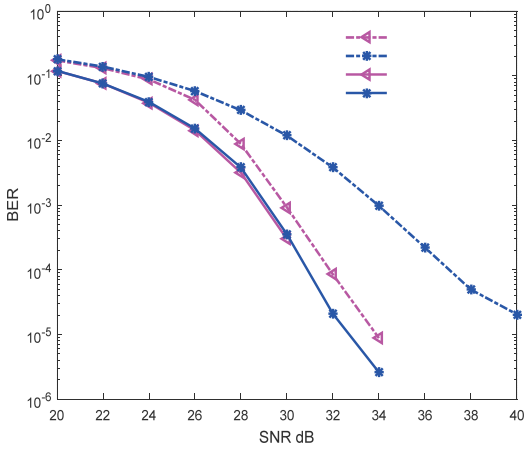

FIGURE 11. Simulation results of the error rate for the two schemes with different signal-to-noise ratios.

The simulation results in Fig. 11 show the BERs of the GAMP-Q-based detection scheme and the LMMSE-Q-based detection scheme for different SNRs and different numbers of transmitting and receiving antennas. The received data detected by the two schemes are quantized by 7-bit ADCs. Because the high-precision quantized bits for 256QAM are usually larger than 12-bit, so 7-bit quantization can reduce the power consumption of the ADCs. If the quantization accuracy is less than 6 bits, the performance of the two schemes is poor, and these methods are impractical. Based on the simulation results, when $N_{\text{T}} = 16$ and $N_{\text{R}} = 256$, the performance of the two schemes is similar, with almost coincident curves. In this case, the system load is low when the number of receiving antennas is much larger than the number of transmitting antennas, so high-precision quantization is not required for effective detection. When $N_{\text{T}} = 128$ and $N_{\text{R}} = 256$ and the SNR is larger than 24 dB, the two schemes exhibit notable differences in performance. For example, when the BER is 10^{-3}, the result of the GAMP-Q-based detection scheme is improved by approximately 11.8% compared with that of the LMMSE-Q-based detection scheme because of the dependence on the detection scheme capability with the large system load and low-precision quantization. Moreover, the GAMP-Q-based scheme, as a novel method of solving the low-precision quantization problem, can eliminate the influence of quantization error caused by low-precision ADCs and obtain better performance than the LMMSE-Q-based scheme applied to the quantization system.

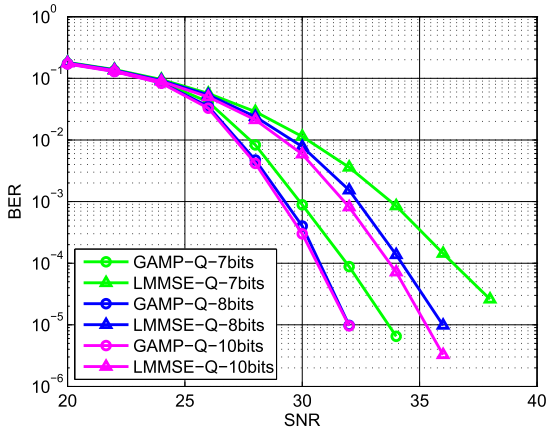

FIGURE 12. Simulation results of the bit error rate for the two schemes with different signal-to-noise ratios when the quantization accuracy is 7 bits, 8 bits or 10 bits, respectively.

Different quantized accuracies have a significant impact on the performance of GAMP and LMMSE based algorithms. Therefore, we show the simulation results in Fig. 12 when the quantized accuracy is 8-bit or 10-bit, respectively. It can be seen that as the number of quantization bit increases, the performance of both algorithms is improved while the proposed GAMP-based algorithm still performs significantly better than the LMMMS-based algorithm, which also shows the general validity of our algorithm at different levels of quantification.

V. CONCLUSION

In this paper, an energy-efficient signal detection scheme for a radar-communication system is proposed based on the GAMP algorithm and low-precision quantization. First, a model of the integrated radar-communication system is designed. Then, a signal detection scheme based on the GAMP algorithm is proposed that only includes matrix-vector multiplication operations and avoids complex matrix inversion. Compared with the conventional LMMSE-based detection scheme, the complexity is reduced from $O(N_{\mathrm{T}}^3 L_{\mathrm{data}})$ to $O(N_{\mathrm{T}} N_{\mathrm{R}} L_{\mathrm{data}})$. The prior probability distribution of the modulated signal and the characteristics of the discrete distribution are used to improve the detection performance. Furthermore, a quantization model is introduced into the output function of the GAMP algorithm for signal detection under the condition of low-precision quantization. The proposed algorithm displayed significant advantages over the LMMSE-based algorithm at the same precision levels. Therefore, energy consumption is further reduced without the performance loss. The energy-efficient scheme proposed in this work will promote practical application of the integrated radar-communication system in future battlefield scenarios.

REFERENCES

[1] L. Han and K. Wu, "Emerging advances in transceiver technology fusion of wireless communication and radar sensing systems," in *Proc. APMC*, Melbourne, VIC, Australia, Dec. 2011, pp. 951–954.
[2] D. Garmatyuk, J. Schuerger, and K. Kauffman, "Multifunctional software-defined radar sensor and data communication system," *IEEE Sensors J.*, vol. 11, no. 1, pp. 99–106, Jan. 2011. doi: 10.1109/JSEN.2010.2052100.
[3] L. Han and K. Wu, "Joint wireless communication and radar sensing systems - state of the art and future prospects," *IET Microw. Antennas Propag.*, vol. 7, no. 11, pp. 876–885, Aug. 2013. doi: 10.1049/iet-map.2012.0450.
[4] S. Quan, W. Qian, J. Guq, and V. Zhang, "Radar-communication integration: An overview," in *Proc. IEEE ICAIT*, Fuzhou, China, Nov. 2014, pp. 98–103. doi: 10.1109/ICAIT.2014.7019537.
[5] G. C. Tavik *et al.*, "The advanced multifunction RF concept," *IEEE Trans. Microw. Theory Techn.*, vol. 53, no. 3, pp. 1009–1020, Mar. 2005. doi: 10.1109/TMTT.2005.843485.
[6] J. A. Molnar, I. Corretjer, and G. Tavik, "Integrated topside–integration of narrowband and wideband array antennas for shipboard communications," in *Proc. IEEE MILCOM*, Baltimore, MD, USA, Nov. 2011, pp. 1802–1807. doi: 10.1109/MILCOM.2011.6127573.
[7] W. H. Weedon, "Phased array digital beamforming hardware development at applied radar," in *Proc. IEEE ARRAY*, Waltham, MA, USA, Oct. 2010, pp. 854–859. doi: 10.1109/ARRAY.2010.5613261.
[8] V. Carulli, R. Nordenberg, A. Fredlund, and A. Ouacha, "New concepts for MRFS evolutionary trends. The M-AESA program: A joint IT-SE capability driven approach," in *Proc. IEEE Radar Conf.*, Rome, Italy, May 2008, pp. 1–8. doi: 10.1109/RADAR.2008.4720973.
[9] Z. Wu, Y. Zhang, and Z. Hang, "A burst SC-FDE scheme for high-speed communication based on radar," in *Proc. IEEE MILCOM*, San Diego, CA, USA, Nov. 2013, pp. 1541–1546. doi: 10.1109/MILCOM.2013.260.
[10] M. Latva-Aho and M. J. Juntti, "LMMSE detection for DS-CDMA systems in fading channels," *IEEE Trans. Commun.*, vol. 48, no. 2, pp. 194–199, Feb. 2000. doi: 10.1109/26.823551.
[11] P. W. Fu and K. C. Chen, "Rate, sub-carrier, and power allocations for multi-carrier CDMA with LMMSE multiuser detection," *IEEE Trans. Wireless Commun.*, vol. 6, no. 5, pp. 1574–1580, May 2007. doi: 10.1109/TWC.2007.360352.
[12] S. Rangan, "Generalized approximate message passing for estimation with random linear mixing," in *Proc. IEEE ISIT*, St. Petersburg, Russia, Jul./Aug. 2011, pp. 2168–2172. doi: 10.1109/ISIT.2011.6033942.
[13] S. Wang, Y. Li, and J. Wang, "Multiuser detection for uplink large-scale MIMO under one-bit quantization," in *Proc. IEEE ICC*, Sydney, NSW, Australia, Jun. 2014, pp. 4460–4465. doi: 10.1109/ICC.2014.6884023.
[14] W. Gruener, J. P. Toernig, and P. J. Fielding, "Active-electronically-scanned-array based radar system features," in *Proc. IET Radar*, Edinburgh, U.K., Oct. 1997, pp. 339–343. doi: 10.1049/cp:19971691.
[15] N. W. Ramsey, C. Mccomb, and D. W. Greig, "Sub-array level simulation of an active electronically scanned array radar for integrated system design," in *Proc. IEEE RadarConf*, Long Beach, CA, USA, Apr. 2002, pp. 243–248. doi: 10.1109/NRC.2002.999726.
[16] G. Golino, "Improved genetic algorithm for the design of the optimal antenna division in sub-arrays: A multi-objective genetic algorithm," in *Proc. IEEE Radar Conf.*, Arlington, VA, USA, May 2005, pp. 629–634. doi: 10.1109/RADAR.2005.1435903.
[17] D. Wang, H. Hu, and Z. Yang, "The Pareto rank algorithm for the division of the sub arrays for the phase array radar," in *Proc. CISP-BMEI*, Datong, China, Oct. 2016, pp. 945–949. doi: 10.1109/CISP-BMEI.2016.7852847.

DE-PING XIA is currently pursuing the Ph.D. degree with Xidian University, Xi'an, China. He is currently a Senior Engineer with the Nanjing Research Institute of Electronics Technology, Nanjing, China. His research interests include the overall technology of the aircraft cutting radar systems, and signal processing.

YU ZHANG (M'07–SM'12) received the B.E. and M.S. degrees in electronics engineering from Tsinghua University, Beijing, China, in 1999 and 2002, respectively, and the Ph.D. degree in electrical and computer engineering from Oregon State University, Corvallis, OR, USA, in 2006. Since 2007, he has been an Assistant Professor with the Research Institute of Information Technology, Tsinghua University, where he is currently an Associate Professor with the Department of Electronic Engineering. His current research interests include the performance analysis and detection schemes for MIMO-OFDM systems over doubly selective fading channels, transmitter and receiver diversity techniques, and channel estimation and equalization algorithm.

PEIXIANG CAI received the B.E. degree from Tsinghua University, Beijing, China, in 2016, where he is currently pursuing the Ph.D. degree. His research interests include communication systems, intelligent transportation systems, information theory, and signal processing.

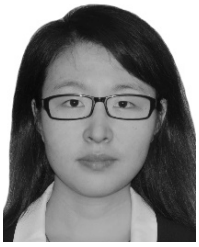

LING HUANG received the B.E. degree from Beihang University, Beijing, China, in 2013, and the Ph.D. degree from Tsinghua University, Beijing, in 2018. She is currently a Researcher with China Fortune Land Development Industrial Investment Co. Ltd., Beijing. Her research interests include communication systems, the Internet of Things, and signal processing.